Taylor & Francis
Taylor & Francis Group

Quality Technology & Quantitative Management

ISSN: (Print) (Online) Journal homepage: https://www.tandfonline.com/loi/ttqm20

Process capability monitoring and change-point analysis for S-type quality characteristic

Mou-Yuan Liao & Chien-Wei Wu

To cite this article: Mou-Yuan Liao & Chien-Wei Wu (2023): Process capability monitoring and change-point analysis for S-type quality characteristic, Quality Technology & Quantitative Management, DOI: 10.1080/16843703.2023.2193365

To link to this article: https://doi.org/10.1080/16843703.2023.2193365

QUALITY TECHNOLOGY & QUANTITATIVE MANAGEMENT
https://doi.org/10.1080/16843703.2023.2193365

Taylor & Francis
Taylor & Francis Group

Process capability monitoring and change-point analysis for S-type quality characteristic

Mou-Yuan Liao[a,b] and Chien-Wei Wu[c]

[a]School of Economics and Management, Huzhou College, Huzhou, China; [b]Department of Data Science and Big Data Analytics, Providence University, Taichung, Taiwan; [c]Department of Industrial Engineering and Engineering Management, National Tsing Hua University, Hsinchu, Taiwan

ABSTRACT

Among various quality assurance activities, process capability indices (PCIs) are recognized as the most effective tools to quantify and evaluate process performance. The one-sided capability index C_{pu} can adequately measure the process capability for processes with a smaller-is-better (S-type) quality characteristic. While focusing on the index C_{pu}, this study constructs a capability control chart to monitor the short-term capability based on the exponentially weighted moving average (EWMA). Simulations have shown that the EWMA capability control chart is adaptive regarding average run length. Further, this study applies change-point analysis to determine whether and when the short-term capability-level changes. Using these two proposed methods, engineers can realize a variety of short-term process capabilities in good time and implement control measures efficiently against a poor long-term process capability.

ARTICLE HISTORY
Received 17 August 2022
Accepted 12 March 2023

KEYWORDS
Change-point; EWMA; process capability

1. Introduction

Process capability indices (PCIs) have been widely used to estimate process capability, understand the company's process performance and select the best supplier based on it. The most well-known PCIs include, C_p, C_{pk}, C_{pm}, C_{pmk}, C_{pu} and C_{pl}. Among these indices, C_p, C_{pk}, C_{pm} and C_{pmk} are designed for measuring the process capability of the nominal-the-best (N-type) quality characteristic while C_{pu} and C_{pl} for measuring the process capability of the S-type quality characteristic and larger-is-better (L-type) quality characteristic, respectively.

PCIs are easy to use and understand (Liao & Pearn, 2017). However, a single index cannot represent specific problems in process performance or provide sufficient information to the production department for improvements (Chang, Wang, & Chen, 2014). Therefore, Spiring (1995) developed a capability control chart for C_{pm} and mentioned its four advantages in practical use: (i) it evidences the capability of the process over its lifetime; (ii) it projects how the estimated process capability varies over the process lifetime; (iii) it reflects any capability changes associated with process changes; and (iv) it incorporates statistic-based inferences into the process capability assessment.

However, real-world applications frequently display S-type quality characteristics, such as noise level, shrinkage and flatness; thus, the C_{pu} index (Kane, 1986) is usually applied to measure the process performances associated with those S-type data. Chen et al. (2007) provided a capability control chart for this index based on the probability limits. They mentioned that their capability

CONTACT Mou-Yuan Liao mouyuanliao@gmail.com School of Economics and Management, Huzhou College, Huzhou, China

control chart could monitor the process capability stability and the process quality. Castagliola & Vännman (2007) constructed capability control charts based on the exponentially weighted moving average (EWMA) for monitoring the indices, C_p, C_{pk}, C_{pm} and C_{pmk}. Further, Castagliola & Vännman (2008) studied optimal parameters for their charts.

These capability control charts developed by Spiring (1995), Castagliola & Vännman (2007) and Chen et al. (2007) were designed to monitor the 'short-term' process capability. In our opinion, the rapid detection and correction of a bad short-term capability is the major merit of process capability control charts. Such short-term correction can prevent a bad 'long-term' process capability. As Zhou et al. (2016) mentioned, quantifying a manufacturing process's current and expected future performance is essential for improving product quality and productivity.

Traditionally, process capability must be analyzed in the in-control Phase, i.e. no assignable cause in the process. Thus, Shewhart control charts are often used to determine whether a cause can be assigned to a process upset. However, in some situations, monitoring the process capability is of interest, although the process is out-of-control. Castagliola & Vännman (2007) explained the need for a capability control chart using a drilling process example. Although the drilling process is naturally unstable due to the manufacturing complexity, the process should be sampled regularly. Further, the capability index for each sample must be calculated to ensure that the diameters of the holes are well within the specification limits and close to the target value.

Inspired by the success of process capability control charts, we propose a control chart for monitoring the process capability of S-type data. The chart is designed based on the EWMA concept. The performance of the proposed chart is compared with the probability-based capability control chart using simulations. Furthermore, we identify the change-point of the capability-level change in a change-point analysis, a powerful change-detection tool in present-day quality control activities.

The remainder of this manuscript is organized as follows. Section 2 briefly reviews the probability-based capability control chart proposed by Chen et al. (2007). Section 3 develops the capability control chart based on the EWMA concept and provides the proper exponential smoothing constants to monitor the short-term capability shift. Section 4 compares the performances of our proposed chart with the probability-based capability control chart in a simulation study. Section 5 adopts the change-point analysis to determine the short-term capability level change. An example is presented in Section 6 to demonstrate the proposed method's applicability. Finally, the conclusions are reported in Section 7.

2. Probability-based capability control chart

The C_{pu} index is defined as (Kane, 1986)

$$C_{pu} = \frac{USL - \mu}{3\sigma} \tag{1}$$

where μ and σ are the process mean and standard deviation, respectively, and USL is the upper specification limit.

If the quality characteristic X follows a Normal distribution, the process yield $\rho\%$ can be expressed as $\rho\% = 100 \times \Phi(3C_{pu})\%$, where $\Phi(\cdot)$ is the cumulative distribution function (CDF) of the standard Normal distribution. The index C_{pu} and the process yield are directly related. Thus, the index C_{pu} precisely measures the process yield. Pearn & Chen (2002) developed a procedure to use samples to determine whether the C_{pu} index value meets the capability requirement. Pearn & Liao (2006) estimated and tested S-type quality characteristics in the presence of measurement error. Kurniati et al. (2015) proposed a sampling scheme for resubmitted lots based C_{pu}. A Markov chain Monte Carlo solution in the Bayesian model was provided by Liao (2016) to test S-type quality characteristics. Liao et al. (2017) assessed the S-type process quality of data involving batch-to-batch

variation. Lee et al. (2002) constructed a sampling scheme by inspecting variables based on the C_{pu}. Liu et al. (2021) proposed an adjustable inspection scheme for lot sentencing based on the C_{pu}. Wu et al. (2021) provided a variable-type skip-lot sampling plan for products with a unilateral specification limit. Recently, Liu et al. (2022) considered an integrated operating mechanism for lot sentencing based on the C_{pu}.

Let us consider that an overall product is manufactured in k continuous batches, each containing N product items. Then, $N \times k$ product items are produced in the whole process. Typically, the practitioners assess the value of the long-term capability index C_{pu} to determine whether these $N \times k$ product items meet the capability requirement. However, to monitor the process capability stability, we must apply the short-term process capability, C_{pu}^S, rather than C_{pu}.

Chen et al. (2007) estimated the short-term process capability by the index $C_{puj}^S = (USL - \mu_j^S)/3\sigma_j^S$, $j \in \{1, 2, \ldots, k\}$, to monitor the jth batch of product items, where μ_j^S and σ_j^S are the process mean and standard deviation, respectively, of the jth batch. However, inspecting all product items is limited by inspection costs. Instead, we must use samples to estimate the indices C_{puj}^S, $j = 1, 2, \ldots, k$.

Further, the sample size can be denoted by n, and the overall sample observations can be represented as $\{x_{ij}; i = 1, 2, \ldots, n, j = 1, 2, \ldots, k\}$. According to Chen et al. (2007), C_{puj}^S, $j = 1, 2, \ldots, k$ are estimated as follows:

$$\tilde{C}_{puj}^S = b_f\left(\frac{USL - \bar{x}_j}{3s_j}\right), j = 1, 2, \ldots, k \tag{2}$$

where $s_j = \sqrt{\Sigma_{i=1}^n (x_{ij} - \bar{x}_j)^2/(n-1)}$ is the standard deviation of the sample observations of jth batch, $\bar{x}_j = \Sigma_{i=1}^n x_{ij}/n$ is the average of the sample observations of j^{th} batch, $b_f = \sqrt{2/(n-1)} \times \Gamma[(n-1)/2]/\Gamma[(n-2)/2]$ is a correction factor and $\Gamma(.)$ is the Gamma function. According to Chen et al. (2007), the upper and lower probability-based control limits are given by

$$UCL_P = b_f\left(\frac{t_{n-1,\alpha/2}(\delta)}{3\sqrt{n}}\right) \tag{3}$$

$$LCL_P = b_f\left(\frac{t_{n-1,1-\alpha/2}(\delta)}{3\sqrt{n}}\right) \tag{4}$$

where $t_{n-1}(\delta)$ is a non-central t distribution with $n-1$ degrees of freedom, $\delta = 3\sqrt{n}C_{pu}^S$ is the non-centrality parameter, $t_{n,\alpha}(\delta)$ is the upper α^{th} percentile of the $t_n(\delta)$ distribution and α is the false alarm rate. Chen et al. (2007) estimated the unknown parameter C_{pu}^S using $\overline{\tilde{C}_{pu}^S} = \sum_{i=1}^k \tilde{C}_{puj}^S/k$. On the other hand, if the capability target value $C_{pu}^{S(0)}$ of the short-term process capability is known, we can substitute it into equations (3) and (4) to obtain the control limits.

3. EWMA capability control chart

Robert (1959) proposed the EWMA statistic for monitoring averaging processes that assign decreasing weights to data further removed in time. However, the data compiled into an EWMA chart should satisfy the normality assumption that the variables $\tilde{C}_{puj}^S$, $j \in \{1, 2, \ldots, k\}$, follow a non-central t distribution (Chen et al., 2007). To assure normality when constructing the EWMA chart, we first transform the $\tilde{C}_{puj}^S$, $j = 1, 2, \ldots, k$, variables into normally distributed variables.

3.1 Derivation of the EWMA capability control limits

As C_{puj}^{S} is a function of μ_j^S and σ_j^S, while $\widetilde{C}_{puj}^{S}$ is a function of $\bar{x}_j$ and s_j^2. Further, we can expand $\widetilde{C}_{puj}^{S}$ by referring to the same technique by Lee et al. (2002) and Pearn & Wu (2013) as the following:

$$\tilde{C}_{puj}^{S}/b_f \approx C_{puj}^{S} - \frac{1}{3\sigma_j}\left(\bar{x}_j - \mu_j\right) - \frac{C_{puj}^{S}}{2\sigma^2{}_j}\left(s^2{}_j - \sigma^2{}_j\right) \tag{5}$$

where $j = 1, 2, \ldots, k$. Now define $U_j = \sqrt{n}(\bar{x}_j - \mu_j)$ and $V_j = \sqrt{n}(s_j^2 - \sigma_j^2)$. Basu's theorem (Basu, 1955) suggests that U_j and V_j are independent. As the first two moments of U_j and V_j exist, they converge to Normal$(0, \sigma_j^2)$ and Normal$(0, 2\sigma_j^4)$, respectively, by the Central Limit Theorem. Therefore, we obtain

$$E\left(\tilde{C}_{puj}^{S}\right) \approx b_f C_{puj}^{S} \tag{6}$$

$$Var\left(\tilde{C}_{puj}^{S}\right) \approx b_f^2\left[\frac{1}{9n} + \frac{\left(C_{puj}^{S}\right)^2}{2n}\right] \tag{7}$$

The sampling distribution of indices $\widetilde{C}_{puj}^{S}$ is approximately normal with parameters $E(\widetilde{C}_{puj}^{S})$ and $Var(\widetilde{C}_{puj}^{S})$. Consequently, the Y_j is given by

$$Y_j = \frac{\tilde{C}_{puj}^{S} - E\left(\tilde{C}_{puj}^{S}\right)}{\sqrt{Var\left(\tilde{C}_{puj}^{S}\right)}},\ j = 1, 2, \ldots, k \tag{8}$$

Notably, every variable Y_j follows the standard Normal distribution. Also, to derive the Y_j, we must replace C_{puj}^{S} by $C_{pu}^{S(0)}$ in equations (6) and (7). Applying the EWMA concept, we get

$$Z_j = (1-\lambda)Z_{j-1} + \lambda Y_j,\ j = 1, 2, \ldots, k \tag{9}$$

where $\lambda \in (0, 1]$ is the exponential smoothing constant and $Z_0 = 0$. In this construct, we monitor Z_j variables in the chart. Their variances are given by

$$Var(Z_j) = \left(\frac{\lambda}{2-\lambda}\right)\left[1 - (1-\lambda)^{2j}\right],\ j = 1, 2, \ldots, k \tag{10}$$

Thus, their control limits are derived as follows:

$$UCL_{Ej} = L\sqrt{Var(Z_j)} = L\sqrt{\left(\frac{\lambda}{2-\lambda}\right)\left[1 - (1-\lambda)^{2j}\right]} \tag{11}$$

$$LCL_{Ej} = -L\sqrt{Var(Z_j)} = -L\sqrt{\left(\frac{\lambda}{2-\lambda}\right)\left[1 - (1-\lambda)^{2j}\right]} \tag{12}$$

where $j = 1, 2, \ldots, k$ and L is a multiplier. For large enough j, we have

$$UCL_E = L\sqrt{\left(\frac{\lambda}{2-\lambda}\right)} \tag{13}$$

$$LCL_E = -L\sqrt{\left(\frac{\lambda}{2-\lambda}\right)} \tag{14}$$

3.2 Parameter determination of the EWMA capability control chart

Equations (13) and (14) include two parameters (L and λ) that must be determined before using the EWMA capability control chart. The parameter λ indicates the weight given to the most recent rational value of the short-term process capability.

While selecting a proper L value (here symbolized by L^*), we consult the ARL. The ARL is the number of points (on average) plotted on a control chart before it indicates an out-of-control condition. For all the short-term process capabilities in control, the ARL is often denoted by ARL_0. This study obtains L using Monte Carlo simulations, converging ARL_0 toward its theoretical value $1/\alpha$. Let M be the number of replicated simulations, $[L_L, L_U]$ be the interval to obtain L^* and $\varepsilon>0$ be a small number denoting the required estimation accuracy. Now all C_{puj}^{S} $(j = 1, 2, \ldots, k)$ equal $C_{pu}^{S(0)}=(USL-\mu^{S(0)})/3\sigma^{S(0)}$, where, $\mu^{S(0)}$ and $\sigma^{S(0)}$ are the mean and standard deviation, respectively.L^* is then obtained by the following procedure:

Step 1: Determine the target $C_{pu}^{S(0)}$, the mean $\mu^{S(0)}$, the sample size n, the false alarm rate α, the exponential smoothing constant λ, the number of replicated simulations M and the required estimation accuracy ε.

Step 2: Letting $L = (L_L + L_U)/2$ with $j = 1$, compute the UCL_E and LCL_E by equations (13) and (14).

Step 3: Generate an n-sized random sample $\{x_i, i = 1, 2, \ldots, n\}$ from normal distribution with $\mu^{S(0)}$ and $\sigma^{S(0)}$ parameters, and substitute the sample into equations (2), (8) and (9) to obtain Z_j. If Z_j belongs to the interval $[LCL_E, UCL_E]$, set $j = j + 1$ and return to Step 2; otherwise, set the run length (RL) to be $j - 1$ and go to Step 4.

Step 4: Iterate Steps 2 and 3 M times, and average the RL values obtained in Step 3. The result is the ARL.

Step 5: If the ARL obtained in Step 4 is present in $[1/\alpha - \varepsilon, 1/\alpha + \varepsilon]$, set $L^* = L$; otherwise, set

$$\begin{cases} L_L = L_L, L_U = (L_L + L_U)/2, if\, ARL > 1/\alpha \\ L_L = (L_L + L_U)/2, L_U = L_U, if\, ARL < 1/\alpha \end{cases} \tag{15}$$

and return to Step 1.

Although the practitioners can apply the above procedure to obtain the control limits efficiently, $C_{pu}^{S(0)}$ is a function of $\mu^{S(0)}$ and $\sigma^{S(0)}$, and we must discuss whether the $\mu^{S(0)}$ value will impact L^*. Recall that Montgomery (2000) suggested a lower C_{pu} limit of 1.25 for existing processes, 1.45 for existing processes on safety, strength, or critical parameters, and 1.60 for new processes. Therefore, we applied Monte Carlo simulation with $M = 100{,}000$ replications to obtain L^* under the parameters $USL = 3$, $C_{pu}^{S(0)} = 1.25$, 1.45 and 1.60; $\mu^{S(0)} = (1/2) \times USL$, $(2/3) \times USL$ and $(5/6) \times USL$; $\sigma^{S(0)}=(USL-\mu^{S(0)})/(3C_{pu}^{S(0)})$; $\lambda = 0.05(0.05)0.95$, $n = 20(10)100$ and $\alpha = 0.02$. Notably, the $\mu^{S(0)}$ range defined here is reasonable because the value $\mu^{S(0)} < (1/2) \times USL$ might cause a negative value in Step 3.

When L^* values round to four decimal places, they become stagnant even though $\mu^{S(0)}$ varies. This implies the parameter $\mu^{S(0)}$ does not influence L^* significantly. Table 1, 2, 3 list those L^* values for reference. It suggests that L^* decreases by increasing n. Moreover, L^* increases with λ and reaches its maximum as λ equals to 0.80, 0.85, 0.90 or 0.95.

Table 1. L^* values for $C_{pu}^{S(0)} = 1.25$ with $\alpha = 0.02$.

	n								
λ	20	30	40	50	60	70	80	90	100
0.05	2.2320	1.9650	1.8401	1.7689	1.7272	1.6952	1.6720	1.6550	1.6433
0.10	2.4818	2.2362	2.1210	2.0527	2.0112	1.9831	1.9610	1.9436	1.9309
0.15	2.6152	2.3756	2.2643	2.2008	2.1556	2.1283	2.1087	2.0917	2.0798
0.20	2.7020	2.4650	2.3538	2.2930	2.2494	2.2204	2.1999	2.1832	2.1710
0.25	2.7672	2.5320	2.4201	2.3560	2.3150	2.2853	2.2640	2.2481	2.2362
0.30	2.8219	2.5854	2.4714	2.4070	2.3618	2.3349	2.3135	2.2959	2.2845
0.35	2.8680	2.6263	2.5118	2.4459	2.4029	2.3742	2.3510	2.3329	2.3205
0.40	2.9050	2.6600	2.5460	2.4784	2.4348	2.4039	2.3810	2.3633	2.3499
0.45	2.9389	2.6908	2.5740	2.5030	2.4589	2.4270	2.4059	2.3879	2.3765
0.50	2.9677	2.7168	2.5969	2.5261	2.4799	2.4480	2.4274	2.4060	2.3941
0.55	2.9932	2.7388	2.6150	2.5457	2.5000	2.4659	2.4430	2.4239	2.4090
0.60	3.0130	2.7576	2.6320	2.5616	2.5129	2.4778	2.4530	2.4355	2.4228
0.65	3.0330	2.7702	2.6459	2.5711	2.5220	2.4911	2.4669	2.4486	2.4329
0.70	3.0409	2.7859	2.6560	2.5824	2.5328	2.5010	2.4754	2.4550	2.4399
0.75	3.0530	2.7937	2.6629	2.5900	2.5397	2.5059	2.4810	2.4624	2.4477
0.80	3.0637	2.8000	2.6690	2.5938	2.5450	2.5113	2.4853	2.4659	2.4489
0.85	3.0630	2.8041	2.6751	2.5984	2.5476	2.5142	2.4890	2.4687	2.4540
0.90	3.0620	2.8050	2.6770	2.5996	2.5498	2.5169	2.4892	2.4719	2.4570
0.95	3.0606	2.8027	2.6719	2.6001	2.5520	2.5170	2.4908	2.4720	2.4570

Table 2. L^*values for $C_{pu}^{S(0)} = 1.45$ with $\alpha = 0.02$.

	n								
λ	20	30	40	50	60	70	80	90	100
0.05	2.2508	1.9749	1.8473	1.7784	1.7320	1.6993	1.6770	1.6580	1.6465
0.10	2.5010	2.2489	2.1298	2.0593	2.0175	1.9865	1.9649	1.9452	1.9342
0.15	2.6305	2.3858	2.2710	2.2059	2.1640	2.1319	2.1133	2.0940	2.0810
0.20	2.7156	2.4760	2.3623	2.2978	2.2565	2.2255	2.2050	2.1879	2.1738
0.25	2.7799	2.5432	2.4287	2.3603	2.3220	2.2895	2.2690	2.2538	2.2376
0.30	2.8329	2.5940	2.4779	2.4090	2.3690	2.3382	2.3187	2.2990	2.2880
0.35	2.8824	2.6390	2.5188	2.4519	2.4055	2.3787	2.3559	2.3386	2.3251
0.40	2.9179	2.6720	2.5527	2.4836	2.4387	2.4090	2.3847	2.3660	2.3539
0.45	2.9536	2.6998	2.5806	2.5097	2.4638	2.4321	2.4084	2.3887	2.3779
0.50	2.9818	2.7249	2.6036	2.5311	2.4840	2.4515	2.4299	2.4108	2.3970
0.55	3.0049	2.7488	2.6235	2.5489	2.5032	2.4689	2.4460	2.4278	2.4126
0.60	3.0250	2.7680	2.6410	2.5640	2.5186	2.4830	2.4590	2.4419	2.4234
0.65	3.0440	2.7810	2.6519	2.5762	2.5300	2.4939	2.4690	2.4490	2.4342
0.70	3.0579	2.7943	2.6619	2.5873	2.5380	2.5041	2.4794	2.4580	2.4423
0.75	3.0667	2.8040	2.6722	2.5951	2.5469	2.5096	2.4850	2.4648	2.4504
0.80	3.0728	2.8110	2.6792	2.6002	2.5490	2.5160	2.4885	2.4690	2.4549
0.85	3.0750	2.8128	2.6800	2.6025	2.5540	2.5167	2.4925	2.4716	2.4587
0.90	3.0781	2.8129	2.6819	2.6060	2.5521	2.5212	2.4942	2.4760	2.4588
0.95	3.0763	2.8100	2.6810	2.6030	2.5540	2.5197	2.4940	2.4747	2.4593

3.3 Optimal exponential smoothing constant

As mentioned in subsection 3.2, when all the short-term process capabilities are in-control, the ARL is often denoted by ARL_0. However, when unstable, the ARL is often renamed as ARL_1. If a short-term process capability has truly shifted, the shift should be detected as soon as possible. Therefore, in a good control chart, a small ARL_1 is desired.

To obtain the optimal exponential smoothing constant λ, we adopt Monte Carlo simulations with 100, 000 replications to obtain the ARLs of the parameters $C_{pu}^{S(0)} = 1.25$, 1.45 and 1.60, $USL = 3$, $\alpha = 0.02$, $n = 20(10)100$, $\lambda = 0.05(0.05)0.95$. In Phase I for constructing EWMA capability control limits LCL_E and UCL_E , the limits can be obtained by substituting the L^* values from Tables 1–3 into

Table 3. L^*values for $C_{pu}^{S(0)} = 1.60$ with $\alpha = 0.02$.

	n								
λ	20	30	40	50	60	70	80	90	100
0.05	2.2630	1.9857	1.8550	1.7825	1.7363	1.7039	1.6771	1.6607	1.6441
0.10	2.5079	2.2552	2.1315	2.0659	2.0190	1.9880	1.9669	1.9488	1.9369
0.15	2.6372	2.3914	2.2751	2.2080	2.1656	2.1350	2.1109	2.0955	2.0829
0.20	2.7249	2.4800	2.3632	2.3000	2.2592	2.2293	2.2056	2.1879	2.1748
0.25	2.7910	2.5452	2.4340	2.3660	2.3207	2.2932	2.2700	2.2552	2.2403
0.30	2.8449	2.5989	2.4817	2.4150	2.3719	2.3401	2.3210	2.3022	2.2890
0.35	2.8890	2.6393	2.5219	2.4530	2.4084	2.3792	2.3583	2.3391	2.3262
0.40	2.9270	2.6769	2.5550	2.4868	2.4409	2.4110	2.3881	2.3692	2.3548
0.45	2.9650	2.7077	2.5827	2.5130	2.4670	2.4349	2.4120	2.3915	2.3778
0.50	2.9866	2.7323	2.6068	2.5345	2.4857	2.4540	2.4319	2.4094	2.3974
0.55	3.0150	2.7530	2.6277	2.5512	2.5040	2.4722	2.4470	2.4280	2.4139
0.60	3.0356	2.7700	2.6430	2.5661	2.5194	2.4843	2.4612	2.4420	2.4249
0.65	3.0493	2.7870	2.6569	2.5816	2.5317	2.4970	2.4708	2.4517	2.4364
0.70	3.0648	2.7992	2.6660	2.5912	2.5410	2.5040	2.4799	2.4590	2.4446
0.75	3.0720	2.8085	2.6762	2.5964	2.5460	2.5150	2.4860	2.4659	2.4504
0.80	3.0810	2.8163	2.6822	2.6063	2.5547	2.5197	2.4899	2.4718	2.4560
0.85	3.0845	2.8219	2.6868	2.6089	2.5563	2.5202	2.4942	2.4752	2.4591
0.90	3.0842	2.8193	2.6868	2.6097	2.5560	2.5220	2.4950	2.4759	2.4597
0.95	3.0819	2.8152	2.6858	2.6066	2.5578	2.5215	2.4970	2.4770	2.4619

equations (13) and (14). In Phase II for monitoring the short-term process capabilities, we varied C_{pu}^{S} from $C_{pu}^{S(0)}$ to $C_{pu}^{S(1)}$, where $C_{pu}^{S(1)}$ is the shifted capability. Denoting $\mu^{S(1)}$ and $\sigma^{S(1)}$ as the mean and standard deviation of the shifted quality observations, respectively, we have $C_{pu}^{S(1)} = (USL - \mu^{S(1)})/3\sigma^{S(1)}$. The $C_{pu}^{S(1)}$ values defined in the simulations are $C_{pu}^{S(1)} = \gamma \times C_{pu}^{S(0)}$, where $\gamma = 0.70(0.05)1.30$. For each Monte Carlo simulation, $\mu^{S(1)}$ was randomly selected from 1.50(0.1)2.5 and posted was determined by $(USL - \mu^{S(1)})/3C_{pu}^{S(1)}$. Then, the sample was randomly produced from Normal distribution with parameters $\mu^{S(1)}$ and $\sigma^{S(1)}$.

Table 4, 5, and 6 list the ARLs of $C_{pu}^{S(0)} = 1.25$, 1.45 and 1.60, respectively. When the short-term process capability does not shift or $C_{pu}^{S(1)} = C_{pu}^{S(0)}$, the ARLs were found very close with $1/\alpha = 50$. This implies that those L^* values in Tables 1–3 are suitable (neither liberal nor conservative) for constructing the control limits.

Further, Table 7, 8, and 9 list the λ values that can produce the smallest ARL_1 than others with the same parameters n and γ of $C_{pu}^{S(0)} = 1.25$, 1.45 and 1.60, respectively. These λ values are optimal for constructing the control limits. Moreover, Table 10, 11, and 12 list the ARL_1 values produced by λ values listed in Tables 7–9, respectively.

From Tables 7–9, without considering the condition $(n, \gamma) = (20, 0.95)$, we observed that the optimal λ value increased with increasing n or amount of shift. From Tables 10–12 for $(n, \gamma) = (20, 0.95)$ or $(30, 0.95)$, the ARL_1 corresponding to the optimal λ showed unreasonable performance, while that in other cases showed reasonable performance and decreased with increasing n or amount of shift.

3.4 Proper exponential smoothing constant

The optimal λ value can be obtained as mentioned in subsection 3.3, but the shift of the short-term process is unpredictable in practice. Thus, this subsection will find the most proper λ value for using the EWMA capability control chart. The method involves averaging the ARL_1 values, denoted by $\overline{ARL_1}$, produced by all λ values when n is fixed, and recommending the λ value that can produce the smallest $\overline{ARL_1}$ to be the proper one.

Table 4. ARL_0 values for $C_{pu}^{S(1)}=C_{pu}^{S(0)}=1.25$ with $\alpha=0.02$.

	n								
λ	20	30	40	50	60	70	80	90	100
0.05	49.932	50.155	49.843	49.792	49.869	49.963	49.894	49.898	50.118
0.10	49.859	49.784	49.983	49.876	49.778	49.849	49.897	50.106	50.301
0.15	50.001	50.097	50.289	50.089	49.750	50.166	50.080	50.037	49.978
0.20	50.188	49.981	49.819	50.041	49.918	50.133	50.115	49.584	49.900
0.25	50.119	50.046	49.886	49.835	49.672	49.652	50.201	49.786	49.945
0.30	49.667	49.968	49.932	50.076	49.882	49.903	49.805	49.869	49.965
0.35	49.903	49.813	50.007	49.994	49.973	50.189	49.896	49.874	49.961
0.40	49.978	49.982	50.037	50.282	50.290	49.972	49.930	49.536	49.712
0.45	50.176	49.893	49.768	50.104	50.016	49.929	50.203	50.261	50.095
0.50	50.109	49.932	49.883	50.095	49.983	50.012	50.211	49.703	50.002
0.55	49.908	49.894	50.032	50.096	50.195	50.156	50.056	50.023	50.096
0.60	49.965	50.162	49.995	50.239	50.213	49.746	50.049	49.922	49.873
0.65	50.433	49.768	50.074	49.967	49.661	50.059	50.035	50.024	50.145
0.70	50.011	50.062	50.100	50.415	50.051	50.327	49.975	49.796	49.767
0.75	50.107	50.109	49.902	50.103	49.734	49.946	50.232	50.423	50.066
0.80	50.150	50.106	49.969	50.071	50.104	49.999	49.793	49.576	49.624
0.85	50.042	50.182	50.181	49.996	49.820	49.785	50.078	49.597	49.780
0.90	49.834	50.159	50.174	49.968	49.973	50.054	49.783	49.894	50.094
0.95	49.961	49.993	49.660	49.978	50.195	49.992	50.187	49.983	49.791

First, we defined a capability shift as a 'small shift' when $0.85 < \gamma < 0.95$ or $1.05 < \gamma < 1.15$ and as a 'large shift' when $0.70 < \gamma < 0.80$ or $1.20 < \gamma < 1.30$. According to this definition, we considered six purposes of using the EWMA capability control chart to find the proper λ values. The six purposes are as follows: (I) process capability shifts up or down, and detection of small shifts or large shifts are equally important; (II) process capability shifts up or down are equally important, but detecting small shifts is more important; (III) process capability shifts up or down are equally important, but detecting large shifts is more important; (IV) detecting small downward shifts and large downward shifts are equally important; (V) detecting small downward shifts is important; and (VI) detecting large downward shifts is important.

Based on different purposes of using the EWMA capability control chart, Table 13, 14, 15, 16, 17, and 18 list the proper λ values and the resulting $\overline{ARL_1}$ values for purposes I – VI, respectively. Notably, the $\overline{ARL_1}$ values for $n=20$ in Table 17 are too large; thus, we recommend using the EWMA capability control chart with a sample size of at least 30.

4. Comparative study

This section compares the proposed EWMA capability control chart with the probability-based control chart (Chen et al., 2007) using Monte Carlo simulations. The key performance measure was the $\overline{ARL_1}$. In the simulations, we set the target value $C_{pu}^{S(0)}=1.25$, 1.45 and 1.60; $USL=3$; $\alpha=0.02$; $n=30(10)100$; $\mu^{S(0)}=2.0$; and $\sigma^{S(0)}=(USL-\mu^{S(0)})/3C_{pu}^{S(0)}$. Further, we applied the proper λ values in Tables 13–18 to determine the EWMA capability control limits. $C_{pu}^{S(1)}$ values were also defined as $C_{pu}^{S(1)}=\gamma\times C_{pu}^{S(0)}$, where $\gamma=0.70(0.05)1.30$. For each Monte Carlo simulation, the $\mu^{S(1)}$ value was randomly selected from 1.50(0.1)2.50 and $\sigma^{S(1)}$ was determined by $(USL-\mu^{S(1)})/3C_{pu}^{S(1)}$. It was followed by randomly producing the sample from Normal distribution with parameters $\mu^{S(1)}$ and $\sigma^{S(1)}$. After 100,000 replications of Monte Carlo simulation, Figure 1(a–f) plots the $\overline{ARL_1}$ values of the two charts for purposes I–VI, respectively.

Further, Figure 1(a–f) demonstrates the following important findings:

Table 5. ARL_0 values for $C_{pu}^{S(1)}=C_{pu}^{S(0)}=1.45$ with $\alpha=0.02$.

	n								
λ	20	30	40	50	60	70	80	90	100
0.05	49.973	49.551	49.602	50.175	50.192	49.972	49.713	50.009	50.102
0.10	50.112	50.174	50.239	49.828	49.888	50.000	49.928	49.771	50.069
0.15	49.749	49.822	49.985	49.923	50.315	49.872	50.138	50.145	49.912
0.20	49.936	50.056	49.835	49.943	49.897	49.987	50.440	49.940	50.169
0.25	49.679	50.086	50.383	49.814	50.085	49.887	49.978	50.195	50.164
0.30	49.832	49.757	49.982	49.558	50.059	50.024	50.000	49.876	50.038
0.35	49.953	50.028	50.000	50.082	49.741	50.127	50.189	50.015	50.117
0.40	49.773	49.883	50.183	49.982	50.028	49.944	50.041	49.988	49.727
0.45	49.998	49.845	50.083	50.300	49.819	49.877	49.904	49.849	49.787
0.50	49.943	49.972	50.294	50.097	49.975	49.898	50.197	49.961	50.063
0.55	50.083	50.159	50.287	50.024	49.769	49.992	50.001	50.055	50.094
0.60	50.057	50.243	50.312	49.660	50.140	49.987	50.228	50.411	49.689
0.65	50.134	49.700	49.916	49.918	49.852	49.990	49.844	49.743	49.713
0.70	50.110	50.145	49.732	49.880	49.992	50.041	50.368	49.861	49.817
0.75	49.686	49.993	49.889	50.044	50.228	49.975	50.289	49.757	50.201
0.80	49.872	50.200	50.045	49.988	50.045	50.128	50.005	49.973	50.013
0.85	49.874	50.133	49.836	49.786	49.884	49.563	50.041	49.830	50.189
0.90	50.172	49.808	50.026	50.044	49.980	50.074	50.164	50.079	50.118
0.95	50.181	49.970	49.723	49.799	49.905	49.914	49.961	50.148	50.118

Table 6. ARL_0 values for $C_{pu}^{S(1)}=C_{pu}^{S(0)}=1.60$ with $\alpha=0.02$.

	n								
λ	20	30	40	50	60	70	80	90	100
0.05	50.190	50.243	50.046	50.035	50.127	50.005	49.706	49.855	49.795
0.10	49.850	50.281	49.819	50.174	49.653	50.059	50.098	49.969	50.075
0.15	49.989	50.004	50.025	49.905	49.937	49.772	49.515	50.013	50.294
0.20	49.972	49.875	49.706	50.231	50.149	50.285	49.759	49.927	49.642
0.25	50.034	49.820	50.030	50.022	49.907	50.141	49.897	50.079	50.126
0.30	50.175	50.041	49.806	49.929	49.747	49.830	50.474	50.207	49.971
0.35	50.111	49.863	49.666	49.782	50.048	49.894	50.149	49.809	50.061
0.40	49.687	49.820	49.880	50.113	49.887	49.992	50.213	50.038	50.002
0.45	50.508	49.956	49.690	50.035	49.886	50.077	50.094	49.746	49.613
0.50	49.535	50.040	50.171	49.963	49.864	49.895	49.886	49.715	49.774
0.55	49.869	49.906	50.298	49.853	49.972	49.914	50.157	49.749	49.937
0.60	50.095	49.620	49.877	50.056	50.030	50.066	50.183	50.161	49.867
0.65	49.723	50.141	50.216	49.993	50.244	49.928	49.988	49.733	49.849
0.70	49.873	49.851	49.648	50.038	50.151	49.891	49.929	49.670	50.245
0.75	49.716	49.839	50.211	49.577	49.668	50.125	49.774	49.935	49.809
0.80	50.147	50.063	49.990	50.054	49.961	49.993	50.014	50.388	49.728
0.85	49.728	50.313	50.144	49.979	50.118	49.794	50.102	50.184	49.749
0.90	49.903	50.051	49.791	50.234	49.601	49.838	49.915	50.155	50.034
0.95	50.011	50.079	49.844	49.526	50.235	49.899	49.996	50.190	50.309

Table 7. Optimal λ values for constructing control limits of $C_{pu}^{S(0)}=1.25$ with $\alpha=0.02$.

	γ												
n	0.70	0.75	0.80	0.85	0.90	0.95	1.00	1.05	1.10	1.15	1.20	1.25	1.30
20	0.25	0.20	0.15	0.10	0.05	0.95	-	0.10	0.15	0.20	0.25	0.30	0.40
30	0.40	0.30	0.20	0.15	0.05	0.05	-	0.10	0.15	0.25	0.30	0.45	0.50
40	0.60	0.40	0.30	0.20	0.10	0.05	-	0.10	0.20	0.30	0.35	0.50	0.65
50	0.75	0.55	0.40	0.25	0.15	0.05	-	0.10	0.25	0.35	0.45	0.60	0.65
60	0.85	0.65	0.45	0.30	0.15	0.05	-	0.10	0.25	0.40	0.50	0.65	0.80
70	0.90	0.75	0.55	0.30	0.15	0.05	-	0.10	0.25	0.45	0.60	0.70	0.80
80	0.90	0.85	0.60	0.40	0.20	0.05	-	0.15	0.30	0.50	0.60	0.80	0.80
90	0.95	0.85	0.70	0.45	0.20	0.10	-	0.15	0.35	0.45	0.60	0.80	0.90
100	0.95	0.90	0.70	0.50	0.25	0.10	-	0.15	0.35	0.50	0.70	0.85	0.90

Table 8. Optimal λ values for constructing control limits of $C_{pu}^{S(0)} = 1.45$ with $\alpha = 0.02$.

	γ												
n	0.70	0.75	0.80	0.85	0.90	0.95	1.00	1.05	1.10	1.15	1.20	1.25	1.30
20	0.25	0.20	0.15	0.10	0.05	0.95	-	0.10	0.15	0.20	0.25	0.30	0.35
30	0.40	0.30	0.20	0.15	0.05	0.05	-	0.10	0.20	0.25	0.30	0.40	0.50
40	0.65	0.40	0.30	0.20	0.10	0.05	-	0.10	0.20	0.30	0.40	0.55	0.65
50	0.75	0.55	0.35	0.25	0.15	0.05	-	0.10	0.25	0.30	0.50	0.60	0.70
60	0.85	0.70	0.45	0.30	0.15	0.05	-	0.10	0.25	0.40	0.55	0.60	0.75
70	0.90	0.75	0.60	0.35	0.15	0.05	-	0.15	0.25	0.45	0.55	0.75	0.85
80	0.90	0.80	0.60	0.40	0.20	0.05	-	0.15	0.25	0.50	0.60	0.80	0.90
90	0.95	0.80	0.70	0.45	0.20	0.10	-	0.15	0.30	0.50	0.70	0.80	0.85
100	0.95	0.95	0.75	0.50	0.25	0.10	-	0.15	0.30	0.55	0.70	0.85	0.95

Table 9. Optimal λ values for constructing control limits of $C_{pu}^{S(0)} = 1.60$ with $\alpha = 0.02$.

	γ												
n	0.70	0.75	0.80	0.85	0.90	0.95	1.00	1.05	1.10	1.15	1.20	1.25	1.30
20	0.25	0.20	0.15	0.10	0.05	0.95	-	0.10	0.15	0.20	0.25	0.30	0.40
30	0.40	0.30	0.20	0.15	0.05	0.05	-	0.10	0.15	0.25	0.35	0.40	0.50
40	0.60	0.40	0.30	0.20	0.10	0.05	-	0.10	0.20	0.30	0.40	0.50	0.60
50	0.75	0.55	0.40	0.25	0.15	0.05	-	0.15	0.25	0.35	0.50	0.60	0.65
60	0.85	0.70	0.45	0.25	0.15	0.05	-	0.15	0.25	0.40	0.55	0.65	0.80
70	0.90	0.80	0.60	0.35	0.20	0.05	-	0.15	0.30	0.40	0.60	0.70	0.85
80	0.90	0.85	0.65	0.40	0.20	0.05	-	0.15	0.35	0.45	0.65	0.75	0.95
90	0.95	0.90	0.70	0.45	0.20	0.10	-	0.15	0.30	0.50	0.70	0.80	0.95
100	0.95	0.85	0.75	0.50	0.25	0.10	-	0.15	0.35	0.60	0.75	0.90	0.90

Table 10. The smallest ARL_1 of $C_{pu}^{S(0)} = 1.25$ with $\alpha = 0.02$.

	γ												
‘	0.70	0.75	0.80	0.85	0.90	0.95	1.00	1.05	1.10	1.15	1.20	1.25	1.30
20	3.306	4.837	7.625	13.622	31.301	92.094	-	17.998	9.536	5.975	4.068	2.935	2.202
30	1.734	2.604	4.141	7.204	15.301	54.963	-	14.718	7.147	4.247	2.764	1.900	1.340
40	1.024	1.710	2.775	4.887	10.166	33.568	-	12.685	5.837	3.306	2.066	1.343	0.890
50	0.590	1.176	2.069	3.709	7.789	24.405	-	11.294	4.969	2.716	1.630	1.003	0.608
60	0.334	0.807	1.594	2.958	6.275	19.574	-	10.267	4.320	2.282	1.317	0.759	0.422
70	0.198	0.558	1.248	2.470	5.327	16.492	-	9.455	3.808	1.967	1.080	0.584	0.296
80	0.113	0.388	0.987	2.097	4.589	14.370	-	8.779	3.438	1.715	0.895	0.450	0.209
90	0.066	0.271	0.782	1.794	4.058	12.778	-	8.178	3.133	1.507	0.750	0.350	0.145
100	0.039	0.189	0.623	1.554	3.625	11.534	-	7.672	2.856	1.334	0.631	0.270	0.102

Table 11. The smallest ARL_1 of $C_{pu}^{S(0)} = 1.45$ with $\alpha = 0.02$.

	γ												
n	0.70	0.75	0.80	0.85	0.90	0.95	1.00	1.05	1.10	1.15	1.20	1.25	1.30
20	3.215	4.755	7.512	13.452	31.230	92.408	-	17.821	9.430	5.857	4.007	2.883	2.154
30	1.691	2.538	4.042	7.041	15.076	54.752	-	14.513	7.043	4.159	2.701	1.854	1.303
40	0.973	1.655	2.711	4.786	9.995	33.154	-	12.523	5.692	3.221	2.017	1.315	0.855
50	0.544	1.124	2.007	3.616	7.663	24.011	-	11.083	4.866	2.640	1.582	0.966	0.584
60	0.309	0.762	1.540	2.900	6.192	19.326	-	10.108	4.247	2.219	1.268	0.729	0.403
70	0.175	0.520	1.196	2.398	5.214	16.250	-	9.260	3.737	1.909	1.039	0.555	0.279
80	0.100	0.356	0.936	2.033	4.493	14.181	-	8.604	3.376	1.658	0.858	0.427	0.194
90	0.056	0.246	0.735	1.734	3.958	12.544	-	8.044	3.065	1.455	0.716	0.330	0.135
100	0.031	0.170	0.584	1.506	3.538	11.286	-	7.519	2.795	1.283	0.596	0.253	0.093

Table 12. The smallest ARL_1 of $C_{pu}^{S(0)} = 1.60$ with $\alpha = 0.02$.

	γ												
n	0.70	0.75	0.80	0.85	0.90	0.95	1.00	1.05	1.10	1.15	1.20	1.25	1.30
20	3.195	4.703	7.429	13.376	31.055	92.506	-	17.677	9.307	5.841	3.959	2.862	2.141
30	1.659	2.499	3.985	6.987	14.964	54.955	-	14.359	6.970	4.092	2.677	1.829	1.277
40	0.953	1.628	2.666	4.724	9.943	33.178	-	12.377	5.630	3.196	1.981	1.291	0.843
50	0.524	1.097	1.968	3.570	7.551	24.075	-	11.062	4.800	2.589	1.553	0.944	0.568
60	0.293	0.738	1.511	2.856	6.110	19.210	-	10.001	4.156	2.193	1.246	0.714	0.387
70	0.164	0.504	1.177	2.363	5.149	16.146	-	9.181	3.704	1.880	1.014	0.542	0.267
80	0.091	0.338	0.915	1.994	4.437	13.997	-	8.477	3.331	1.634	0.839	0.414	0.184
90	0.050	0.232	0.718	1.702	3.911	12.419	-	7.937	3.009	1.434	0.695	0.316	0.126
100	0.029	0.158	0.565	1.472	3.473	11.213	-	7.430	2.748	1.266	0.582	0.244	0.087

Table 13. Proper λ values for purpose I.

	$C_{pu}^{S(0)}$=1.25		$C_{pu}^{S(0)}$=1.45		$C_{pu}^{S(0)}$=1.60	
n	λ	$\overline{ARL_1}$	λ	$\overline{ARL_1}$	λ	$\overline{ARL_1}$
20	0.10	20.363	0.05	20.620	0.10	20.820
30	0.05	10.611	0.05	10.513	0.05	10.501
40	0.10	7.294	0.10	7.214	0.10	7.161
50	0.10	5.697	0.10	5.614	0.10	5.591
60	0.15	4.735	0.15	4.664	0.15	4.614
70	0.15	4.066	0.15	3.991	0.15	3.954
80	0.15	3.588	0.20	3.515	0.15	3.457
90	0.20	3.183	0.20	3.109	0.20	3.069
100	0.20	2.873	0.20	2.797	0.20	2.760

Table 14. Proper λ values for purpose II.

	$C_{pu}^{S(0)}$=1.25		$C_{pu}^{S(0)}$=1.45		$C_{pu}^{S(0)}$=1.60	
n	λ	$\overline{ARL_1}$	λ	$\overline{ARL_1}$	λ	$\overline{ARL_1}$
20	0.05	35.563	0.05	35.975	0.05	36.418
30	0.05	17.740	0.05	17.598	0.05	17.587
40	0.05	12.297	0.05	12.131	0.05	12.100
50	0.10	9.590	0.10	9.459	0.10	9.427
60	0.10	7.971	0.10	7.857	0.10	7.774
70	0.10	6.928	0.10	6.792	0.10	6.719
80	0.15	6.141	0.15	6.020	0.15	5.921
90	0.15	5.522	0.15	5.405	0.15	5.328
100	0.15	5.018	0.15	4.910	0.15	4.857

Table 15. Proper λ values for purpose III.

	$C_{pu}^{S(0)}$=1.25		$C_{pu}^{S(0)}$=1.45		$C_{pu}^{S(0)}$=1.60	
n	λ	$\overline{ARL_1}$	λ	$\overline{ARL_1}$	λ	$\overline{ARL_1}$
20	0.20	4.272	0.20	4.197	0.20	4.161
30	0.30	2.464	0.30	2.403	0.30	2.372
40	0.40	1.685	0.40	1.636	0.40	1.608
50	0.50	1.217	0.50	1.172	0.55	1.148
60	0.60	0.899	0.60	0.861	0.60	0.841
70	0.65	0.676	0.65	0.645	0.65	0.626
80	0.70	0.517	0.75	0.490	0.70	0.475
90	0.75	0.401	0.75	0.376	0.75	0.363
100	0.80	0.313	0.80	0.293	0.75	0.282

Table 16. Proper λ values for purpose IV.

	$C_{pu}^{S(0)}$=1.25		$C_{pu}^{S(0)}$=1.45		$C_{pu}^{S(0)}$=1.60	
n	λ	$\overline{\text{ARL}_1}$	λ	$\overline{\text{ARL}_1}$	λ	$\overline{\text{ARL}_1}$
20	0.05	32.720	0.05	33.164	0.05	33.611
30	0.05	14.977	0.05	14.852	0.05	14.856
40	0.05	9.753	0.05	9.615	0.05	9.603
50	0.10	7.260	0.10	7.173	0.10	7.142
60	0.10	5.825	0.10	5.745	0.10	5.680
70	0.10	4.942	0.10	4.839	0.10	4.786
80	0.15	4.276	0.15	4.191	0.15	4.119
90	0.15	3.772	0.15	3.681	0.15	3.627
100	0.20	3.358	0.20	3.270	0.15	3.249

Table 17. Proper λ values for purpose V.

	$C_{pu}^{S(0)}$=1.25		$C_{pu}^{S(0)}$=1.45		$C_{pu}^{S(0)}$=1.60	
n	λ	$\overline{\text{ARL}_1}$	λ	$\overline{\text{ARL}_1}$	λ	$\overline{\text{ARL}_1}$
20	0.05	59.102	0.05	60.050	0.05	60.969
30	0.05	26.056	0.05	25.868	0.05	25.892
40	0.05	16.612	0.05	16.382	0.05	16.379
50	0.05	12.418	0.05	12.231	0.05	12.208
60	0.10	10.032	0.10	9.906	0.10	9.794
70	0.10	8.472	0.10	8.293	0.10	8.205
80	0.10	7.351	0.10	7.225	0.10	7.146
90	0.10	6.494	0.10	6.371	0.10	6.305
100	0.15	5.865	0.15	5.744	0.15	5.685

Table 18. Proper λ values for purpose VI.

	$C_{pu}^{S(0)}$=1.25		$C_{pu}^{S(0)}$=1.45		$C_{pu}^{S(0)}$=1.60	
n	λ	$\overline{\text{ARL}_1}$	λ	$\overline{\text{ARL}_1}$	λ	$\overline{\text{ARL}_1}$
20	0.15	5.335	0.15	5.252	0.15	5.196
30	0.25	2.865	0.25	2.799	0.25	2.757
40	0.35	1.901	0.35	1.844	0.40	1.819
50	0.45	1.332	0.50	1.285	0.50	1.259
60	0.60	0.953	0.60	0.910	0.60	0.885
70	0.65	0.690	0.65	0.653	0.65	0.632
80	0.70	0.509	0.75	0.479	0.70	0.461
90	0.75	0.382	0.75	0.354	0.75	0.340
100	0.80	0.288	0.75	0.267	0.75	0.255

(1) The $\overline{\text{ARL}_1}$s of the two charts both decrease as the n increases; this implies that large samples can both increase the abilities of the two charts for detecting the capability shift.
(2) The $\overline{\text{ARL}_1}$s of the two charts decrease as the $C_{pu}^{S(0)}$ increases, implying that both charts have better abilities to detect the capability shift on higher capability targets.
(3) The $\overline{\text{ARL}_1}$s of the EWMA capability control chart are all smaller than those of the probability-based for purposes I and III, and also for purpose II but with an exception for $n = 30$. Thus, we can conclude that the EWMA capability control chart outperforms the probability-based ones in monitoring the capability shift overall.
(4) For purpose IV, the $\overline{\text{ARL}_1}$s of the probability-based capability control chart are smaller than those of the EWMA for n approximately smaller than 80. This implies that the EWMA capability control chart only outperforms the probability-based ones in monitoring a downward capability shift when $n \geq 90$.

(5) For purpose V, the $\overline{\text{ARL}_1}$s of the probability-based capability control chart are smaller than those of the EWMA for n smaller than 60. This implies that the EWMA capability control chart can outperform the probability-based ones in monitoring a small downward capability shift when $n \geq 60$.
(6) For purpose VI, all the $\overline{\text{ARL}_1}$s of the probability-based capability control chart are smaller than those of the EWMA. This implies that the probability-based capability control chart outperforms the EWMA ones in monitoring the large downward capability shift.

In summary, we recommend the EWMA capability control chart for monitoring capability shift because of its better detection ability than the probability-based capability control chart. Although the EWMA capability control chart is also adaptive to monitor the downward capability shift, considering sufficient samples can further improve its ability.

5. Change-point detection

A capability control chart suggests a significant shift from the target capability when the point estimator of the capability moves outside the control limits. However, a capability shift from the target does not imply a 'change' in the capability level. For instance, suppose that a point estimate of the capability in one batch lies outside the capability control limits, but in other batches, all lie inside the capability control limits, which makes it challenging to conclude a change in the capability level of the process. A change-point analysis is needed to determine whether or when the capability level has changed.

In the change-point analysis, we assume that all C^S_{puj} values for $j = 1, 2, \ldots, r$ are equal to $C^{S(0)}_{pu}$ and that all C^S_{puj} values for $j = r+1, r+2, \ldots, k$ are equal to $C^{S(1)}_{pu}$. The variables $Y_j, j = 1, 2, \ldots, r$ determined by equation (8), follow the standard Normal distribution, but not the variables Y_j, $j = r+1, r+2, \ldots, k$. Therefore, we can apply the testing hypotheses proposed by Hawkins (1977):

$$H_0 : Y_j \sim \text{Normal}(0,1) \text{ for } j = 1, 2, \ldots, k \tag{16}$$

$$H_1 : Y_j \sim \text{Normal}(0,1) \text{for } j = 1, 2, \ldots, r \text{ and } Y_j \sim \text{Normal}(\psi, 1) \text{ for } j = r+1, r+2, \ldots, k \tag{17}$$

where $\psi \neq 0$. Further, we conducted a likelihood ratio test (LRT) described in Hawkins et al. (2003) to determine whether to reject or accept H_0. As the variances of $Y_j, j = 1, 2, \ldots, k$, all equal one, the test statistic in the LRT is derived as follows:

$$T_{\max,w} = \max_{1 \leq g \leq w-1} \left| T_{gw} \right| \text{ for } w = 1, 2, \ldots, k \tag{18}$$

where

$$T_{g,w} = \sqrt{\frac{g(w-g)}{w}} \left[\frac{(\bar{Y}_g - \bar{Y}'_g)}{\sqrt{V_{gw}/(w-2)}} \right] \tag{19}$$

$V_{gw} = \Sigma_{i=1}^{g}(Y_i - \bar{Y}_g)^2 + \Sigma_{i=g+1}^{w}(Y_i - \bar{Y}'_g)^2$, $\bar{Y}_g = \Sigma_{i=1}^{g} Y_i/g$ and $\bar{Y}'_g = \Sigma_{i=g+1}^{w} Y_i/(w-g)$. For reliable testing, the first 9 observations should be in control (Hawkins et al., 2003). Thus, w must not be less than 10. Consequently, equation (18) is modified as $T_{\max,w} = \max_{1 \leq g \leq w-1} |T_{g,w}|$ for $w = 10, 11, \ldots, k$. If the test statistic $T_{\max,w}$ is sufficiently large, then we reject H_0. Defining the threshold of large-enough $T_{\max,w}$ as q, the significance level α for testing must satisfy $P(T_{\max,w} > q) \leq \alpha$. However, owing to the complicated distribution of $T_{\max,w}$, the exact value of q is challenging to compute. Hawkins et al. (2003) adopted Monte Carlo simulations to obtain the

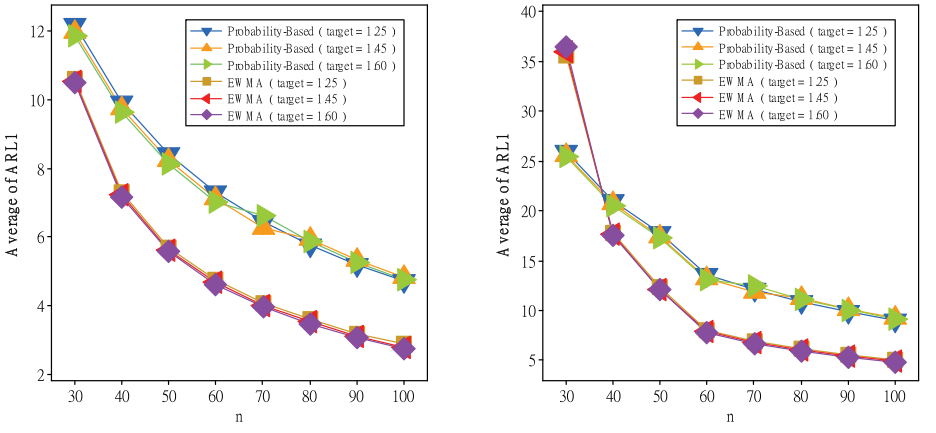

(a) $\overline{ARL_1}$ values for purpose I. (b) $\overline{ARL_1}$ values for purpose II.

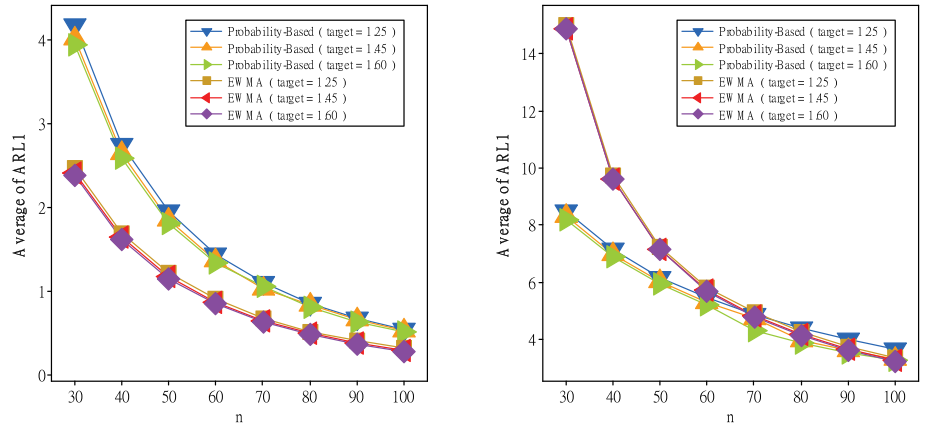

(c) $\overline{ARL_1}$ values for purpose III. (d) $\overline{ARL_1}$ values for purpose IV.

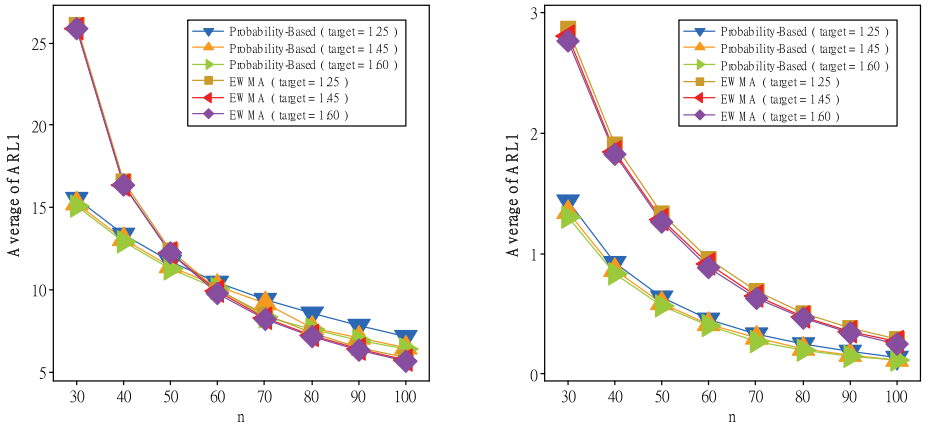

(e) $\overline{ARL_1}$ values for purpose V. (f) $\overline{ARL_1}$ values for purpose VI.

Figure 1. (a) $\overline{ARL_1}$ values for purpose I. (b) $\overline{ARL_1}$ values for purpose II. (c) $\overline{ARL_1}$ values for purpose III. (d) $\overline{ARL_1}$ values for purpose IV. (e) $\overline{ARL_1}$ values for purpose V. (f) $\overline{ARL_1}$ values for purpose VI.

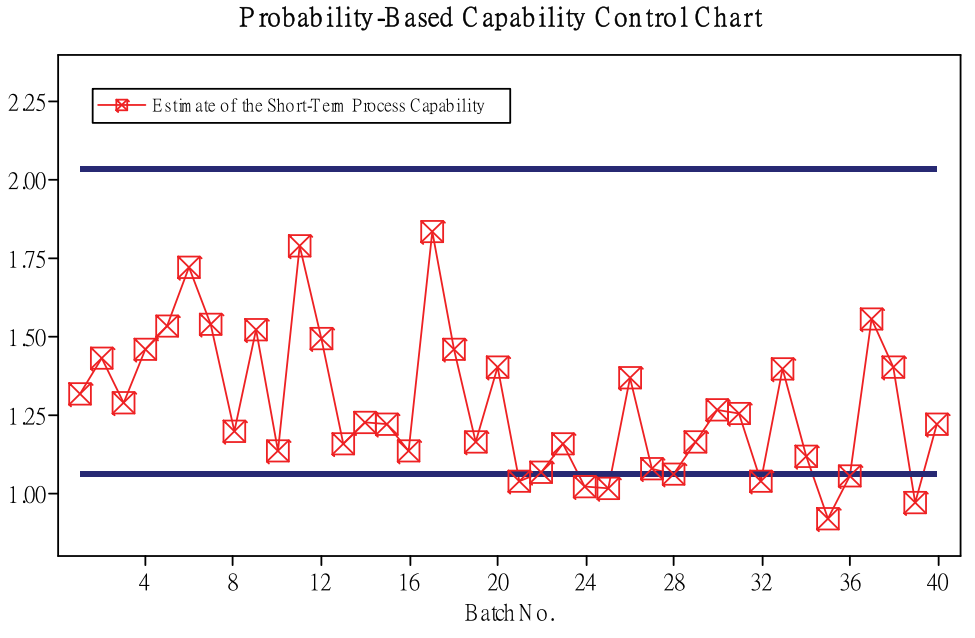

Figure 2. Capability shift detection by the probability-based capability control chart.

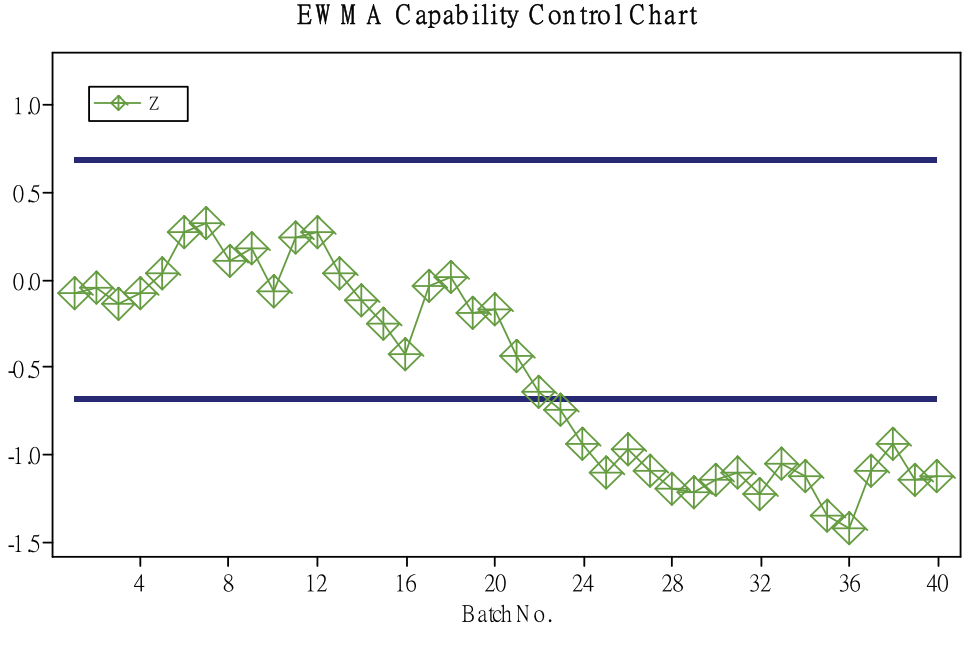

Figure 3. Capability shift detection by the EWMA capability control chart.

best solution, such as listed in Table 19. If $T_{\max,w}$ first exceeds q at the time point w_0, then $\hat{r} = \arg \max_{1 \le g \le w_0 - 1} |T_{g,w_0}|$ is estimated as the change point; that is, the capability level begins to change at point $\hat{r}$+1.

Table 19. Threshold q for change-point analysis under various w and α.

	α				
w	0.02	0.01	0.005	0.002	0.001
10	4.371	4.928	5.511	6.340	7.023
11	3.908	4.424	4.958	5.697	6.284
12	3.677	4.167	4.664	5.350	5.890
13	3.530	3.997	4.468	5.110	5.608
14	3.424	3.875	4.326	4.931	5.397
15	3.344	3.780	4.211	4.786	5.229
16	3.281	3.704	4.121	4.671	5.093
17	3.228	3.642	4.047	4.576	4.977
18	3.183	3.587	3.981	4.494	4.885
19	3.146	3.542	3.926	4.425	4.799
20	3.115	3.503	3.880	4.367	4.730
22	3.060	3.437	3.800	4.264	4.610
24	3.019	3.386	3.736	4.187	4.514
26	2.985	3.343	3.685	4.119	4.440
28	2.957	3.308	3.643	4.065	4.375
30	2.933	3.279	3.609	4.024	4.324
35	2.888	3.223	3.539	3.937	4.223
40	2.855	3.184	3.492	3.873	4.147
45	2.832	3.152	3.454	3.828	4.095
50	2.811	3.128	3.426	3.791	4.053
60	2.785	3.094	3.383	3.737	3.989
70	2.765	3.071	3.355	3.702	3.946
80	2.752	3.052	3.333	3.677	3.918
90	2.741	3.040	3.318	3.656	3.895
100	2.735	3.030	3.307	3.640	3.785
125	2.717	3.011	3.281	3.611	3.844
150	2.710	2.997	3.264	3.591	3.821
175	2.703	2.993	3.257	3.579	3.804
200	2.700	2.985	3.248	3.570	3.794

6. Example

In this section, we generate sample observations to demonstrate the proposed methods. The parameters were defined as $k = 40$, $n = 30$, $USL = 3$, $C_{pu}^{S(0)} = 1.45$, $\alpha = 0.02$, $\lambda = 0.15$. At the beginning, we let $\mu^{S(0)} = 2.0$, $\sigma^{S(0)} = (USL - \mu^{S(0)})/3C_{pu}^{S(0)} = 0.2299$ to obtain $L^* = 2.3858$. Then, we obtained the EWMA capability control limits as [−0.6794, 0.6794]. Further, the probability-based control limits, [1.0597, 2.0377], were calculated by equations (3) and (4). When a batch's process capability did not shift, $\mu^{S(0)}$was randomly selected from 1.50(0.1)2.50, $\sigma^{S(0)}$ was calculated by $(USL - \mu^{S(0)})/3C_{pu}^{S(0)}$, and the sample observations of this batch were randomly sampled from Normal distribution with parameters $\mu^{S(0)}$ and $\sigma^{S(0)}$. On the contrary, when a batch's process capability shifted, $\mu^{S(1)}$ was randomly selected from 1.75(0.1)2.75, $\sigma^{S(1)}$ was calculated by $(USL - \mu^{S(1)})/3C_{pu}^{S(1)}$ and the sample observations of this batch were randomly sampled from Normal distribution with parameters $\mu^{S(1)}$ and $\sigma^{S(1)}$.

Assuming that the capability level changed from $C_{pu}^{S(0)}$ to $C_{pu}^{S(1)} = 0.85 \times C_{pu}^{S(0)}$ at $r = 20$ implies that the last twenty batches' process capabilities all shifted to $C_{pu}^{S(1)}$. Based on the parameter values defined above, sample observations were generated for the overall batches. The mean and standard deviation of each batch's sample observations are listed in Tables 20 and 21. Further, the probability-based and the EWMA capability control charts were applied to detect the capability shifts. The corresponding results are shown in Figures 2 and 3.

The first alarm signal for a shift of the probability-based and the EWMA capability control charts was at the 21st and 23rd batches, respectively. As expected, the probability-based capability control chart first alerts because of its performance. However, the probability-based capability control chart

Table 20. The mean of the sample observations.

Batch No.	1	2	3	4	5	6	7	8	9	10
$\bar{x}$	1.4662	2.2166	1.7304	1.9145	2.1280	1.5365	2.0579	2.0079	2.0405	1.7333
Batch No.	11	12	13	14	15	16	17	18	19	20
$\bar{x}$	2.1088	2.3177	1.4801	1.6293	2.0972	1.5250	2.1244	2.2063	2.2500	2.5329
Batch No.	21	22	23	24	25	26	27	28	29	30
$\bar{x}$	2.5476	2.1585	2.5613	2.3451	2.2371	1.7789	2.2539	1.8553	2.6416	2.6701
Batch No.	31	32	33	34	35	36	37	38	39	40
$\bar{x}$	2.0262	2.7686	2.3151	1.9534	2.0498	2.4448	2.5443	1.9836	2.5767	1.9730

Table 21. The standard deviation of the sample observations.

Batch No.	1	2	3	4	5	6	7	8	9	10
s	0.3779	0.1775	0.3197	0.2410	0.1843	0.2759	0.1986	0.2690	0.2044	0.3620
Batch No.	11	12	13	14	15	16	17	18	19	20
s	0.1616	0.1480	0.4253	0.3631	0.2405	0.4213	0.1547	0.1762	0.2094	0.1082
Batch No.	21	22	23	24	25	26	27	28	29	30
s	0.1415	0.2561	0.1228	0.2085	0.2430	0.2900	0.2250	0.3492	0.1001	0.0846
Batch No.	31	32	33	34	35	36	37	38	39	40
s	0.2520	0.0724	0.1591	0.3043	0.3359	0.1708	0.0950	0.2353	0.1418	0.2730

only warned at the 21st, 24th, 25th, 32nd, 35th, 36th and 39th batches, and unfortunately, could not correctly find out the overall shifts. The EWMA capability control chart was the second fastest to alert a shift, but it was only two batches behind the probability-based capability control chart. Besides, the EWMA capability control chart correctly estimated all the shifts after the 23rd batch. This result reveals that the EWMA capability control chart could perform well in detecting a capability shift.

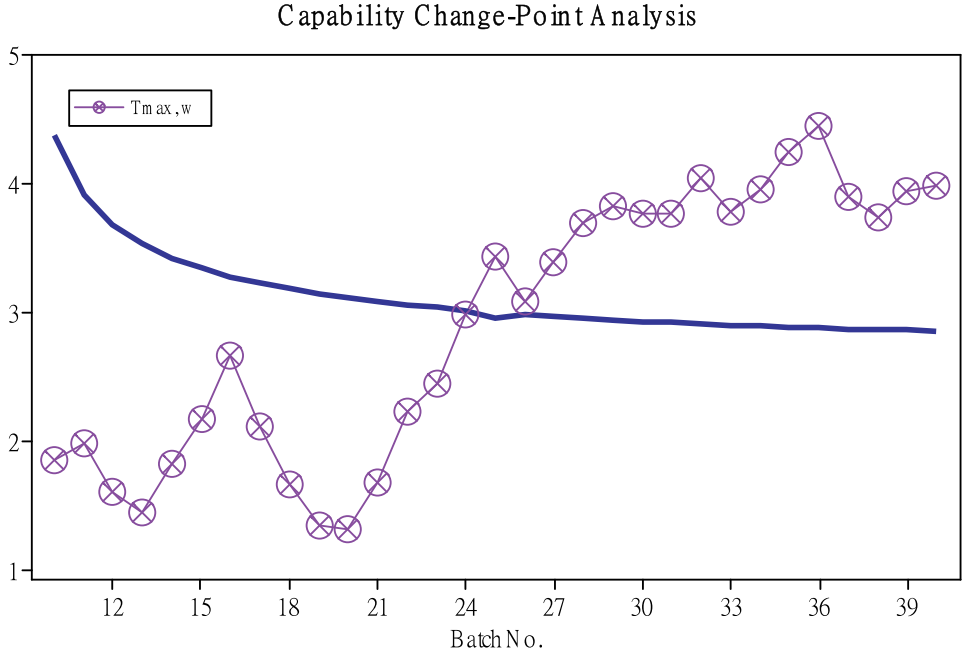

Figure 4. Capability level change detection by the change-point analysis.

Table 22. The $|T_{g,w_0}|$ values of each batch under $w_0 = 25$.

Batch No.	1	2	3	4	5	6
$\|T_{g,w_0}\|$	0.0686	0.2486	0.0941	0.3706	0.7616	1.5186
Batch No.	7	8	9	10	11	12
$\|T_{g,w_0}\|$	1.8817	1.5171	1.8538	1.4224	2.3324	2.6959
Batch No.	13	14	15	16	17	18
$\|T_{g,w_0}\|$	2.2888	2.0694	1.8581	1.5005	2.7037	3.2314
Batch No.	19	20	21	22	23	24
$\|T_{g,w_0}\|$	2.9124	3.4384	2.7548	2.2299	2.0644	1.3661

In the change-point analysis, $T_{\max,w} = 3.4384$ first exceeded its threshold $q = 2.952$ at the 25th batch (see Figure 4); that is, $w_0 = 25$. It can be said that change-point analysis very early alerts the capability-level change. The $|T_{g,w_0}|$ values of $T_{\max,w_0}$ are listed in Table 22, which reveals that its maximum was observed on the 20th batch when $w_0 = 25$; that is, $\hat{r} = 20$. The change-point analysis accurately estimated the change-point of capability level. Compared with those capability control charts, the merit of change-point analysis is informing the capability-level change. Therefore, the capability control chart and the change-point analysis are complementary for monitoring the process capability.

7. Conclusions

PCI is a critical measure to assess whether the process results fit the product specifications. S-type quality characteristics are very commonly encountered in daily applications. The process performances of these data are usually measured by C_{pu}. This study proposed the EWMA capability control chart for monitoring the capability shift because the index C_{pu} interests the processing community. Furthermore, we provided the proper exponential smoothing constants for application. Simulations showed that the EWMA capability control chart is adaptive for a sample size of at least 30. Besides, the simulation results indicated that for monitoring a downward capability shift, sufficient samples are necessary to improve the detection ability.

Moreover, we presented a change-point analysis for detecting capability-level change in the process. This analysis provided further information on monitoring the short-term process capability. Compared with capability control charts, the merit of change-point analysis was informing the capability-level changes if the capability had indeed changed. Further, the practitioner can be guided toward restoring or holding the process capability by inspecting the signals of the EWMA capability control chart and the change-point analysis simultaneously.

This study assumed only one change point for the change-point analysis. The proposed method would be inapplicable in monitoring the short-term process capabilities with multiple change points. Thus, introducing multiple change-point analyses into capability monitoring problems is an exciting avenue for further study.

Disclosure statement

No potential conflict of interest was reported by the authors.

Notes on contributors

Mou-Yuan Liao is currently a professor in the Department of Data Science and Big Data Analytics, Providence University. He received his PhD degree in Industrial Engineering and Management from National Chiao Tung University (NCTU) in 2007 and the MS degree in Statistics from Cheng Kung University (NCKU) in 2002. His research interests include statistical process control, statistical computing, machine learning and data mining.

Chien-Wei Wu is currently a professor in the Department of Industrial Engineering and Engineering Management at National Tsing Hua University (NTHU). He received his PhD degree in Industrial Engineering and Management with Outstanding Ph. D. Student Award from National Chiao Tung University (NCTU) in 2004, the MS degree in Statistics from NTHU in 2002 and the BS degree in Applied Mathematics with the Phi Tao Phi Honor from National Chung Hsing University (NCHU) in 2000. He worked for National Taiwan University of Science and Technology (NTUST) and Feng Chia University (FCU) before he joined NTHU. He has received Dr Ta-You Wu Memorial Award (Outstanding Young Researcher Award) from the National Science Council (NSC) in 2011 and Outstanding Young Industrial Engineer Award from the Chinese Institute of Industrial Engineers (CIIE) in 2011, Excellent Research Award in 2011 and Excellent Teaching Award in 2012 from NTUST and Outstanding Research Award from NSC in 2021. His research interests include quality engineering and management, statistical process control, process capability analysis, applied statistics and data analysis.

References

Basu, D. (1955). On statistics independent of a complete sufficient statistic. *Sankhyā*, *15*(4), 377–380.

Castagliola, P., & Vännman, K. (2007). Monitoring capability indices using an EWMA approach. *Quality and Reliability Engineering International*, *23*(7), 769–790.

Castagliola, P., & Vännman, K. (2008). Average run length when monitoring capability indices using EWMA. *Quality and Reliability Engineering International*, *24*(8), 941–955.

Chang, T. C., Wang, K. J., & Chen, K. S. (2014). Capability performance analysis for processes with multiple characteristics using accuracy and precision. *Proceedings of the Institution of Mechanical Engineers, Part B: Journal of Engineering Manufacture*, *228*(5), 766–776.

Chen, K. S., Huang, H. L., & Huang, C. T. (2007). Control charts for one-sided capability indices. *Quality & Quantity*, *41*(3), 413–427. https://doi.org/10.1007/s11135-006-9013-y

Hawkins, D. M. (1977). Testing a sequence of observations for a shift in location. *Journal of the American Statistical Association*, *72*(357), 180–186. https://doi.org/10.1080/01621459.1977.10479935

Hawkins, D. M., Qiu, P. H., & Kang, C. W. (2003). The change point model for statistical process control. *Journal of Quality Technology*, *35*(4), 355–366. https://doi.org/10.1080/00224065.2003.11980233

Kane, V. E. (1986). Process capability indices. *Journal of Quality Technology*, *18*(1), 41–52. https://doi.org/10.1080/00224065.1986.11978984

Kurniati, N., Yeh, R. H., & Wu, C. W. (2015). A sampling scheme for resubmitted lots based on one-sided capability indices. *Quality Technology & Quantitative Management*, *12*(4), 501–515.

Lee, J. C., Hung, H. N., Pearn, W. L., & Kuengion, T. L. (2002). The distribution of the estimated process yield index *Spk*. *Quality and Reliability Engineering International*, *18*(2), 111–116.

Lee, A. H. I., Wu, C. W., & Wang, Z. H. (2018). The construction of a modified sampling scheme by variables inspection based on the one-sided capability index. *Computers & Industrial Engineering*, *122*(8), 87–94.

Liao, M. Y. (2016). Markov chain Monte Carlo in Bayesian models for testing gamma and lognormal S-type process qualities. *International Journal of Production Research*, *54*(24), 7491–7503.

Liao, M. Y., & Pearn, W. L. (2017). Modified weighted standard deviation index for adequately interpreting a supplier's lognormal process capability. *Proceedings of the Institution of Mechanical Engineers, Part B: Journal of Engineering Manufacture*, *223*(3), 999–1008.

Liao, M. Y., Wu, C. W., & Wen, S. H. (2017). Assessing S-type process quality of data involving batch-to-batch variation. *Journal of Testing and Evaluation*, *45*(4), 1425–1435.

Liu, S. W., Wu, C. W., & Tsai, Y. H. (2021). An adjustable inspection scheme for lot sentencing based on one-sided capability indices. *Applied Mathematical Modelling*, *96*(August), 766–778.

Liu, S. W., Wu, C. W., & Wang, Z. H. (2022). An integrated operating mechanism for lot sentencing based on process yield. *Quality Technology & Quantitative Management*, *19*(2), 139–152.

Montgomery, D. C. (2000). *Introduction to statistical quality control* (4th ed.). John Wiley and Sons.

Page, E. S. (1954). Continuous inspection scheme. *Biometrika*, *41*(1–2), 100–115.

Pearn, W. L., & Chen, K. S. (2002). One-sided capability indices and: Decision making with sample information. *International Journal of Quality & Reliability Management*, *19*(3), 221–245.

Pearn, W. L., & Liao, M. Y. (2006). One-sided process capability assessment in the presence of measurement errors. *Quality and Reliability Engineering International*, *22*(7), 771–785.

Pearn, W. L., & Wu, C. H. (2013). Supplier selection for multiple-characteristics processes with one-sided specifications. *Quality Technology & Quantitative Management*, *10*(1), 133–139.

Robert, S. W. (1959). Control chart tests based on geometric moving averages. *Technometrics*, *1*(3), 239–250.

Spiring, F. A. (1995). Process capability: A total quality management tool. *Total Quality Management*, *6*(1), 21–33.
Wu, C. W., Lee, A. H. I., & Huang, Y. S. (2021). A variable-type skip-lot sampling plan for products with a unilateral specification limit. *International Journal of Production Research*, *59*(14), 4140–4156.
Zhou, X., Jiang, P., & Wang, Y. (2016). Sensitivity analysis-based dynamic process capability evaluation for small batch production runs. *Proceedings of the Institution of Mechanical Engineers, Part B: Journal of Engineering Manufacture*, *230*(10), 1855–1869.